Registration of N-D Images by Blur Invariants

Jan Flusser and Jiří Boldyš *

Institute of Information Theory and Automation
Academy of Sciences of the Czech Republic
Pod vodárenskou věží 4, 182 08 Prague 8, Czech Republic
{flusser,boldys}@utia.cas.cz

Abstract. Registration of monomodal as well as multimodal images is a fundamental task in medical image processing. In this paper, the attention is paid to landmark matching. We present a new class of invariants defined on a volumetric neighborhood of a landmark. They are invariant to convolving the image by arbitrary centrosymmetric function and to image translation. Since the method operates directly on the image grey values, it is particularly designed for multitemporal N-D images of the same modality. The images are assumed to be degraded by an unknown amount of blur, introduced by the point-spread function of the imaging system.

1 Introduction

Registration of monomodal as well as multimodal images is a fundamental task in medical image processing [23]. Regardless of the modalities involved and of the image dimensions, the registration usually consists of the four following steps.

Landmark detection. In medical imaging, landmarks can be significant anatomical points easily locatable by an expert [17], [18], [19] or feature points of distinguished geometry detected automatically (corners, blood vessel junctions, points of maximum curvature, inflex points, etc.) [34], [31], [32], [1], [28], [29]. Landmarks can be also artificial objects of invasive or noninvasive character [20], [9], [22].

Landmark matching. In this step, the mutual correspondence between the reference landmark set and the landmarks in the sensed image(s) is to be established. Common difficulty here is that there could be some landmarks having no corresponding counterparts in the other frame(s). Matching methods can be based on parameter clustering [30], graph matching [14], relaxation [26], [33] correlation-like techniques [25], [2], [4] taking into account the landmark neighborhood or hybrid invariant approaches [34], [10], [35], [8], [6].

* This work has been supported by the grant No. 624178-3 of the Grant Agency of the Czech Ministry of Health. The authors thank to Dr. Igor Hollander for providing the CT data.

Estimation of the mapping model. In this stage, the type and parameters of spatial transform are to be determined. In case of rigid deformations, a linear transform model, the coefficients of which are calculated via least-square technique, is commonly used [15]. When non-rigid deformations are present, local mapping [11], [12], [13], radial basis functions and thin-plate splines [21], [27], [3] are the most popular solutions.

Resampling and transformation. Finally, the sensed image is transformed over the reference one according to the above mapping model. An appropriate resampling technique (nearest neighbor, linear or cubic interpolation) [24], [16] is employed to find image values in non-integer coordinates.

In this paper, the attention is paid to landmark matching. We present a new class of invariants defined on a volumetric neighborhood of a landmark. The method is particularly designed for N-D images ($N \geq 2$) of the same modality, which were taken under different conditions and at different times. The images are assumed to be degraded by an unknown amount of blur, introduced by the point-spread function (PSF) of the imaging system. The novelty of the presented method is the invariance of the proposed features under convolution with an arbitrary centrosymmetric PSF.

2 The Invariants

In this Section, we introduce the moment-based features invariant to convolution and translation. These invariants will be later calculated on an N-D neighborhood of each landmark and will be used for landmark matching.

We introduce basic notation and some important definitions first.

Notation: For $N \geq 2$, $x_i \in \mathcal{R}$, $p_i \in \mathcal{N}_0$, $k_i \in \mathcal{N}_0$ we introduce N-dimensional vector of coordinates

$$\mathbf{x} \equiv (x_1, \cdots, x_N),$$

N-dimensional vectors of parameters

$$\mathbf{p} \equiv (p_1, \cdots, p_N), \qquad \mathbf{k} \equiv (k_1, \cdots, k_N)$$

and the following notation:

$$\mathbf{dx} \equiv dx_1 \cdots dx_N,$$

$$|\mathbf{p}| \equiv \sum_{i=1}^{N} p_i,$$

$$\mathbf{x}^{\mathbf{p}} \equiv \prod_{i=1}^{N} x_i^{p_i},$$

$$\binom{\mathbf{p}}{\mathbf{k}} \equiv \prod_{i=1}^{N} \binom{p_i}{k_i}.$$

Definition 1: By N-dimensional *image function* (or *image*) we understand any real function $f(\mathbf{x}) \in L_1(\mathcal{R}^N)$ which is non-zero on bounded support and whose integral is positive.

Definition 2: *Central moment* $\mu_{\mathbf{p}}^{(f)}$ of order $|\mathbf{p}|$ of the image $f(\mathbf{x})$ is defined as

$$\mu_{\mathbf{p}}^{(f)} = \int_{R^N} (\mathbf{x} - \mathbf{x_t})^{\mathbf{p}} f(\mathbf{x}) \mathbf{dx}, \tag{1}$$

where $\mathbf{x_t}$ denotes the centroid of $f(\mathbf{x})$.

Each sensed image $g(\mathbf{x})$ which we want to register is assumed to be a blurred and shifted version of the original image $f(\mathbf{x})$:

$$g(\mathbf{x} - \mathbf{a}) = (f * h)(\mathbf{x}), \tag{2}$$

where $h(\mathbf{x})$ is an unknown centrally symmetric PSF of the imaging system and $*$ denotes N-D convolution. Any functional I whose domain is a space of N-D functions and that fulfills the invariance constraint $I(g) = I(f)$ regardless of h is called *blur invariant*.

Theorem 1: Let $f(\mathbf{x})$ be an image function. Let us define the following function $C^{(f)} : \mathcal{N}_0^N \to \mathcal{R}$.
If $|\mathbf{p}|$ is even then

$$C(\mathbf{p})^{(f)} = 0.$$

If $|\mathbf{p}|$ is odd then

$$C(\mathbf{p})^{(f)} = \mu_{\mathbf{p}}^{(f)} - \frac{1}{\mu_{\mathbf{0}}^{(f)}} \sum_{\substack{\mathbf{0} \leq \mathbf{n} \leq \mathbf{p} \\ 0 < |\mathbf{n}| < |\mathbf{p}|}} \binom{\mathbf{p}}{\mathbf{n}} C(\mathbf{p} - \mathbf{n})^{(f)} \cdot \mu_{\mathbf{n}}^{(f)}. \tag{3}$$

Then $C(\mathbf{p})$ is a blur invariant for any $\mathbf{p}$.

For the proof of Theorem 1 we refer to our recent work [5]. Obviously, any $C(\mathbf{p})$ is a translation invariant too.

Applying the definition formula (3), we can construct the invariants of any order and express them in explicit forms. By permutations of indeces in the formulas listed below, it is possible to obtain a set of all invariants of this kind of the 3rd and 5th orders:

3rd order:

$$C(3, 0, \cdots, 0) = \mu_{30\cdots0},$$

$$C(2, 1, 0, \cdots, 0) = \mu_{210\cdots0},$$

$$C(1, 1, 1, 0, \cdots, 0) = \mu_{1110\cdots0}.$$

5th order:

$$C(5,0,\cdots,0)=\mu_{50\cdots0}-\frac{10\mu_{30\cdots0}\mu_{20\cdots0}}{\mu_{0\cdots0}},$$

$$C(4,1,0,\cdots,0)=\mu_{410\cdots0}-\frac{2}{\mu_{0\cdots0}}(3\mu_{210\cdots0}\mu_{20\cdots0}+2\mu_{30\cdots0}\mu_{110\cdots0}),$$

$$C(3,2,0,\cdots,0)=$$

$$\mu_{320\cdots0}-\frac{1}{\mu_{0\cdots0}}(3\mu_{120\cdots0}\mu_{20\cdots0}+\mu_{30\cdots0}\mu_{020\cdots0}+6\mu_{210\cdots0}\mu_{110\cdots0}),$$

$$C(3,1,1,0,\cdots,0)=\mu_{3110\cdots0}-\frac{1}{\mu_{0\cdots0}}(\mu_{30\cdots0}\mu_{0110\cdots0}$$

$$+3\mu_{210\cdots0}\mu_{1010\cdots0}+3\mu_{2010\cdots0}\mu_{110\cdots0}+3\mu_{1110\cdots0}\mu_{20\cdots0}),$$

$$C(2,2,1,0,\cdots,0)=\mu_{2210\cdots0}-\frac{1}{\mu_{0\cdots0}}(\mu_{0210\cdots0}\mu_{20\cdots0}+4\mu_{1110\cdots0}\mu_{110\cdots0}$$

$$+\mu_{2010\cdots0}\mu_{020\cdots0}+2\mu_{120\cdots0}\mu_{1010\cdots0}+2\mu_{210\cdots0}\mu_{0110\cdots0}),$$

$$C(1,1,1,1,1,0,\cdots,0)=\mu_{111110\cdots0}-\frac{1}{\mu_{0\cdots0}}(\mu_{001110\cdots0}\mu_{110\cdots0}$$

$$+\mu_{010110\cdots0}\mu_{1010\cdots0}+\mu_{011010\cdots0}\mu_{10010\cdots0}+\mu_{01110\cdots0}\mu_{100010\cdots0}$$

$$+\mu_{100110\cdots0}\mu_{0110\cdots0}+\mu_{101010\cdots0}\mu_{01010\cdots0}+\mu_{10110\cdots0}\mu_{010010\cdots0}$$

$$+\mu_{110010\cdots0}\mu_{00110\cdots0}+\mu_{11010\cdots0}\mu_{001010\cdots0}+\mu_{1110\cdots0}\mu_{000110\cdots0}).$$

3 Numerical Experiments

The aim of the following experiments is to test whether the proposed invariants (3) could be used in registration of 3-D CT images as a tool for landmark or object matching. We do not discuss neither landmark detection nor object segmentation here, we rather refer to the literature cited in Section I. To evaluate the performance and numerical properties of the invariants (3), the experiments demonstrating their invariance to blurring, robustness to additive random noise and the discrimination power were carried out.

Data. A 3-D CT image of a human head of the size 256^3 voxels was chosen as our test data. Two perpendicular slices of it (157th axial, 130th sagittal) are shown in Fig. 1. We chose one of clearly visible "compact" objects (we denoted it as P) and we extracted it from the "background" via thresholding (see Fig. 2). Note that P is still a greylevel object, it was not binarized. Its size is $45 \times 63 \times 38$ voxels.

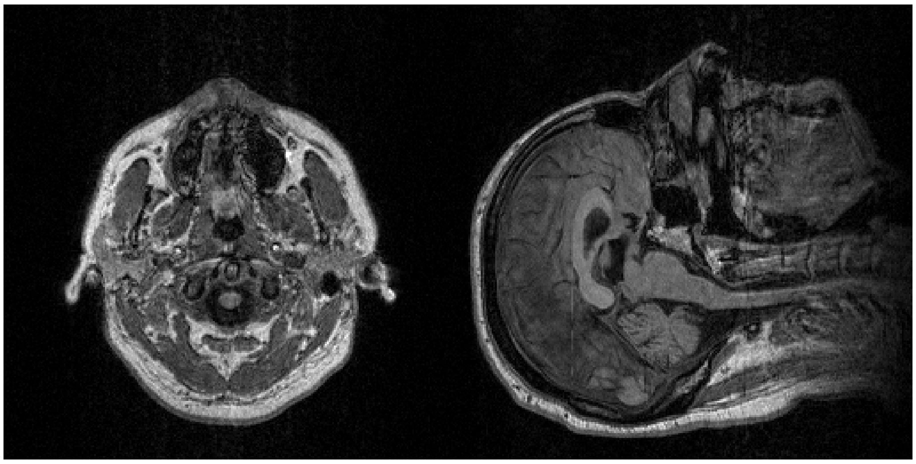

Fig. 1. Original CT data of a human head: 157th axial slice (left) and 130th sagittal slice (right)

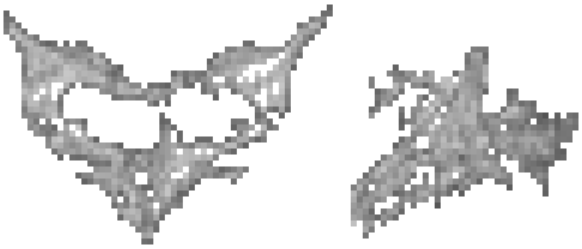

Fig. 2. Extracted test object P: Horizontal (left) and sagittal (right) slices

Test of invariance. The aim of this test was to prove the invariance of (3) experimentally. Theorem 1 guarantees the invariance in continuous domain. In discrete domain it might be disturbed namely due to the three following factors: boundary error when calculating discrete convolution of the PSF and the region of interest, quantization error when the blurred image is converted to a finite number of grey levels and round off errors of calculations.
In this experiment, the image of P was convolved with various blurring masks and 31 invariants up to the 5th order of the blurred images were calculated and compared with those of P. The results are summarized in Table 1. As a distance measure between the blurred image and P, the sum of relative deviations σ_r of all calculated invariants was used. It is obvious from Table 1 that the values of the invariants are sufficiently stable in all examined cases. On the other hand, the invariants of image *(i)* are significantly different that shows a good discrimination power.

Test of robustness. In case the blurred image is corrupted by the additive zero-mean random noise $n(\mathbf{x})$,

$$g(\mathbf{x}) = (f * h)(\mathbf{x}) + n(\mathbf{x}), \tag{4}$$

the invariants can be processed as random variables.
In our experiment, the image P was corrupted by Gaussian noise whose STD varied from 5 to 50. On each level of noise, 10 different realizations of noisy image were generated and their invariants were calculated. Then the relative distance of the mean of the invariants from the original σ_r was calculated on each noise level. The results are shown in Fig. 3. Even in the worst case (STD $= 50$), σ_r of the noisy image is about hundred times smaller than that of image *(i)* from the previous experiment.
The above results indicate the robustness of the invariants is sufficiently high. However, we did not compare it with the robustness of other matching methods (cross-correlation, ℓ_1-norm, etc.) because it is not relevant – the other methods are not invariant to blurring.

Registration test. In this experiment, we investigated the possibility to register two 3-D images which are differently blurred. Such a task might appear for instance in monomodal multitemporal imaging. For this purpose the original CT image was convolved with a $3\times3\times3$ centrosymmetric mask. The task was to register this blurred data with the original image of P. The registration parameters (translation in three dimensions) were determined as the global minimum of σ_r. The registration error was zero in one dimension and 1 pixel in the other two dimensions that is an acceptable accuracy.

4 Conclusion

In this paper we dealt with a registration problem of N-D images which are degraded by blurring. We proposed a new class of features invariant to convolution that can be used for landmark or object matching. Such kind of features has been reported never before. We proved by experiments that the invariants are

Table 1. Relative deviations of the 3rd and 5th-order invariants for differently blurred versions of P. Blurring masks: *(a)* – none, *(b)* – $3 \times 3 \times 3$ averaging, *(c)* – $5 \times 5 \times 5$ averaging, *(d)* – $5 \times 5 \times 5$ Gaussian, *(e)* – $5 \times 5 \times 5$ Gaussian + additive random noise of STD = 10, *(f)* – $5 \times 5 \times 5$ Gaussian + additive random noise of STD = 30, *(g)* and *(h)* – $3 \times 3 \times 3$ masks containing also negative coefficients, *(i)* – different part of original CT image of the same size as P. σ_r – relative distance from P.

	(a)	(b)	(c)	(d)	(e)	(f)	(g)	(h)	(i)
C(3,0,0)	0	0.0003	0.0010	0.0004	0.0005	0.1016	0.0003	0.0001	5.3642
C(0,3,0)	0	0.0100	0.0291	0.0137	0.0593	0.1948	0.0104	0.0037	55.1335
C(0,0,3)	0	0.0021	0.0039	0.0022	0.0080	0.0087	0.0021	0.0008	1.0392
C(2,1,0)	0	0.0001	0.0005	0.0002	0.0057	0.0894	0.0001	0.0000	0.7343
C(2,0,1)	0	0.0002	0.0004	0.0002	0.0050	0.0086	0.0002	0.0001	0.9836
C(1,2,0)	0	0.0025	0.0080	0.0036	0.1785	0.3285	0.0026	0.0009	1.7666
C(1,0,2)	0	0.0213	0.0105	0.0093	0.4966	0.8208	0.0221	0.0078	24.9922
C(0,2,1)	0	0.0033	0.0099	0.0046	0.0028	0.0031	0.0034	0.0012	0.0836
C(0,1,2)	0	0.0168	0.0492	0.0229	0.0538	0.0451	0.0174	0.0061	2.6735
C(1,1,1)	0	0.0002	0.0004	0.0002	0.0868	0.1378	0.0002	0.0001	10.4776
C(5,0,0)	0	0.0005	0.0016	0.0007	0.0284	0.0124	0.0005	0.0002	25.8427
C(0,5,0)	0	0.0092	0.0252	0.0124	0.1511	0.0883	0.0096	0.0035	219.0866
C(0,0,5)	0	0.0007	0.0024	0.0010	0.0108	0.0114	0.0007	0.0002	1.0224
C(4,1,0)	0	0.0003	0.0009	0.0004	0.0046	0.0522	0.0003	0.0001	7.5114
C(4,0,1)	0	0.0001	0.0002	0.0001	0.0019	0.0294	0.0001	0.0000	1.6222
C(1,4,0)	0	0.0132	0.0418	0.0191	0.2161	0.0660	0.0137	0.0049	17.8268
C(1,0,4)	0	0.0116	0.0202	0.0010	0.3472	0.1301	0.0120	0.0043	18.2438
C(0,4,1)	0	0.0014	0.0040	0.0019	0.0186	0.0470	0.0015	0.0005	1.7342
C(0,1,4)	0	0.0038	0.0129	0.0055	0.0129	0.0486	0.0039	0.0013	3.9817
C(3,2,0)	0	0.0052	0.0166	0.0076	0.0854	0.2211	0.0054	0.0019	14.7070
C(3,0,2)	0	0.0041	0.0150	0.0064	0.0615	0.6525	0.0042	0.0015	4.0744
C(2,3,0)	0	0.0026	0.0092	0.0040	0.0223	0.3889	0.0027	0.0009	13.4883
C(2,0,3)	0	0.0033	0.0101	0.0046	0.0174	0.1143	0.0034	0.0012	0.6863
C(0,2,3)	0	0.0161	0.0532	0.0237	0.0676	0.2564	0.0167	0.0059	4.9538
C(0,3,2)	0	0.0188	0.0552	0.0257	0.0388	0.1171	0.0195	0.0065	13.8835
C(3,1,1)	0	0.0038	0.0139	0.0060	0.3574	1.1624	0.0040	0.0014	50.6478
C(1,3,1)	0	0.0028	0.0128	0.0051	0.2234	0.5301	0.0030	0.0010	22.1300
C(1,1,3)	0	0.0026	0.0123	0.0048	0.1512	0.6055	0.0027	0.0010	14.2231
C(2,2,1)	0	0.0276	0.0816	0.0379	0.3192	2.2262	0.0286	0.0102	3.3118
C(2,1,2)	0	0.0019	0.0072	0.0030	0.0663	0.2445	0.0019	0.0008	9.8724
C(1,2,2)	0	0.0068	0.0120	0.0071	0.5522	1.8652	0.0071	0.0025	9.2733
σ_r	0	0.1932	0.5213	0.2356	3.6513	10.6082	0.2006	0.0705	561.3717

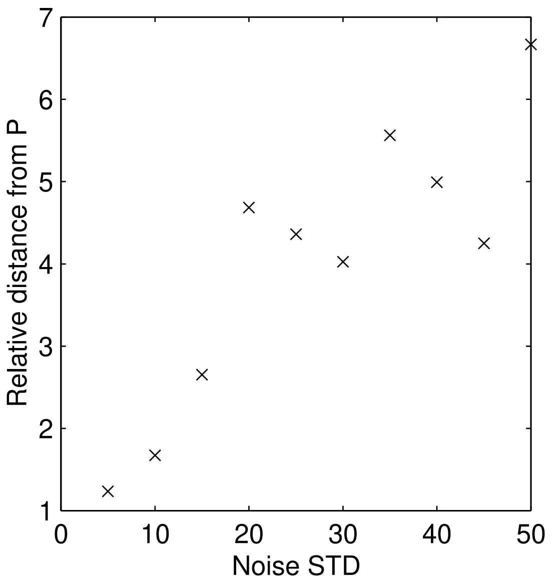

Fig. 3. Behaviour of the invariants under image corruption by additive random noise

sufficiently robust and discriminative and that they are able to register blurred 3-D tomographic images with subvoxel accuracy.

However, all experiments presented in this paper were performed on simulated data only. Both blur and noise were introduced by computer, not by a real imaging, and no geometric distortions were present. Application of this method in clinical practise would require to make the invariants at least rotationally independent. Unfortunatelly, this is not straightforward. Recently we have proposed a solution in 2-D that is based on complex moments [7]. General blur-rotation invariants in N-D are, however, still under investigation.

References

1. T. Ault and M. W. Siegel. Frameless patient registration using ultrasonic imaging: A preliminary study. *Image Guided Surgery*, 1:94–102, 1995.
2. P. K. Banerjee and A. W. Toga. Image alignment by integrated rotational and translational transformation matrix. *Phys. Med. Biol.*, 39:1969–1988, 1994.
3. M. H. Davis, A. Khotanzad, D. P. Flamig, and S. E. Harms. A physics-based coordinate transformation for 3-D image matching. *IEEE Trans. Medical Imaging*, 16(3):317–328, 1997.
4. E. De Castro and C. Morandi. Registration of translated and rotated images using finite Fourier transforms. *IEEE Trans. Pattern Analysis and Machine Intelligence*, 5:700–703, 1987.
5. J. Flusser and J. Boldyš. Invariants to linear imaging system in N dimensions. *J. of Mathematical Imaging and Vision*, submitted.

6. J. Flusser and T. Suk. Degraded image analysis: An invariant approach. *IEEE Trans. Pattern Analysis and Machine Intelligence*, 20(6):590–603, 1998.
7. J. Flusser and B. Zitová. Combined invariants to linear filtering and rotation. *Intl. J. Pattern Recognition Art. Intell.*, 13(7), 1999 (to appear).
8. J. Flusser. Object matching by means of matching likelihood coefficients. *Pattern Recognition Letters*, 16:893–900, 1995.
9. K. P. Gall and L. J. Verhey. Computer-assisted positioning of radiotherapy patients using implanted radioopaque fiducials. *Med. Phys.*, 20:1152–1159, 1993.
10. A. Goshtasby. Template matching in rotated images. *IEEE Trans. Pattern Analysis and Machine Intelligence*, 7:338–344, 1985.
11. A. Goshtasby. Piecewise linear mapping functions for image registration. *Pattern Recognition*, 19(6):459–466, 1986.
12. A. Goshtasby. Piecewise cubic mapping functions for image registration. *Pattern Recognition*, 20(5):525–533, 1987.
13. A. Goshtasby. Image registration by local approximation methods. *Image and Vision Computing*, 6(4):255–261, 1988.
14. A. Goshtasby and G. C. Stockman. Point pattern matching using convex hull edges. *IEEE Trans. Systems, Man, and Cybernetics*, 15(5):631–637, 1985.
15. A. Goshtasby, G. C. Stockman, and C. V. Page. A region-based approach to digital image registration with subpixel accuracy. *IEEE Trans. Geoscience and Remote Sensing*, 24(3):390–399, 1986.
16. G. J. Grevera and J. K. Udupa. An objective comparison of 3-D image interpolation methods. *IEEE Trans. Medical Imaging*, 17(4):642–652, 1998.
17. D. L. G. Hill, D. J. Hawkes, J. E. Crossman, M. J. Gleeson, T. C. S. Cox, E. C. M. L. Bracey, A. J. Strong, and P. Graves. Registration of MR and CT images for skull base surgery using pointlike anatomical features. *Brit. J. Radiol.*, 64:1030–1035, 1991.
18. D. L. G. Hill, D. J. Hawkes, and C. R. Hardingham. The use of anatomical knowledge to register 3D blood vessel data derived from DSA with MR images. In *Medical Imaging: Image Processing*, volume SPIE 1445, pages 348–357. SPIE Press, Bellingham, WA, 1991.
19. D. L. G. Hill, D. J. Hawkes, S. E. M. Hussain, C. F. Ruff, and G. P. Robinson. Accurate combination of CT and MR data of the head: Validation and applications in surgical and therapy planning. *Comput. Med. Imag. Graphics*, 17:357–363, 1993.
20. L. Lemieux and R. Jagoe. Effect of fiducial marker localization on stereotactic target coordinate calculation in CT slices and radiographs. *Phys. Med. Biol.*, 39:1915–1928, 1994.
21. H. Lester and S. R. Arridge. A survey of hierarchical non-linear medical image registration. *Pattern Recognition*, 32(1):129–149, 1999.
22. G. Q. Maguire, M. Noz, H. Rusinek, J. Jaeger, E. L. Kramer, J. J. Sanger, and G. Smith. Graphics applied to medical image registration. *IEEE Comp. Graphics Appl.*, 11:20–28, 1991.
23. J. B. A. Maintz and M. A. Viergever. A survey of medical image registration. *Medical Image Analysis*, 2(1):1–36, 1998.
24. J. A. Parker, R. V. Kenyon, and D. E. Troxel. Comparison of interpolating methods for image resampling. *IEEE Trans. Medical Imaging*, 2(1):31–39, 1983.
25. W. K. Pratt. Correlation techniques of image registration. *IEEE Trans. Aerospace and Electronic Systems*, 10:353–358, 1974.
26. S. Ranade and A. Rosenfeld. Point pattern matching by relaxation. *Pattern Recognition*, 12:269–275, 1980.

27. K. Rohr, H. S. Stiehl, R. Sprengel, W. Beil, T. M. Buzug, J. Weese, and M. H. Kuhn. Nonrigid registration of medical images based on anatomical point landmarks and approximating thin-plate splines. In T. Lehmann, I. Scholl, and K. Spitzer, editors, *Proc. Aachener Workshop 1996: Bildverarbeitung für die Medizin.*, pages 41–46, Hamburg, Germany, 1996.
28. K. Rohr. On 3D differential operators for detecting point landmarks. *Image and Vision Computing*, 15:21–233, 1997.
29. K. Rohr. Extraction of 3D anatomical point landmarks based on invariance principles. *Pattern Recognition*, 32:3–15, 1999.
30. G. Stockman, S. Kopstein, and S. Benett. Matching images to models for registration and object detection via clustering. *IEEE Trans. Pattern Analysis and Machine Intelligence*, 4(3):229–241, 1982.
31. J. Thirion. Extremal points: Definition and application to 3D image registration. In *Proc. Computer Vision and Pattern Recognition*, pages 587–592. IEEE Computer Society Press, Los Alamitios, CA, 1994.
32. J. Thirion. New feature points based on geometric invariants for 3D image registration. *Int. J. Computer Vision*, 18:121–137, 1996.
33. J. Ton and A. K. Jain. Registering Landsat images by point matching. *IEEE Trans. Geoscience and Remote Sensing*, 27(5):642–651, 1989.
34. N. Vujovic and D. Brzakovic. Establishing the correspondence between control points in pairs of mammographic images. *IEEE Trans. Image Processing*, 6(10):1388–1399, 1997.
35. R. Y. Wong and E. L. Hall. Scene matching with invariant moments. *Computer Graphics and Image Processing*, 8:16–24, 1978.